Research Article

A convolutional neural networks approach using X-Ray absorption images for studying granular activated carbon

Jeamichel Puente Torres[1] · Rafael Trujillo Codorniu[1] · Rene López Baracaldo[2] · Harold Crespo Sariol[3] · Thayset Mariño Peacok[3] · Jan Yperman[4] · Peter Adriaensens[4] · Robert Carleer[4] · Ángel Brito Sauvanell[3]

Received: 9 April 2020 / Accepted: 4 November 2020 / Published online: 26 November 2020

Abstract
X-ray methods have proven to be reliable, accurate and sensitive techniques to study activated carbons. The studying of granular activated carbon (GAC) samples through X-ray digital radiographic images using Deep Learning, more specifically convolutional neural networks (CNN) class of model, has been explored. Results were compared to hand-engineered characterization using X-Ray absorption method (XRA). It was proved that CNNs represent a fast and reliable analytical tool for indirect information on the chemical and physical characteristics of GACs. The proposed method opens possibilities for the application of Deep Learning based models on radiographic images for the characterization and comparison of exhausted and virgin porous materials.

Keywords Deep learning · Neural network · Activated carbon · XRA · Digital image processing

1 Introduction

Activated carbons (ACs) are specific and versatile adsorbents because of their extended surface area, high pore volume, porous structure and specific surface functional groups [1–3]. X-Ray absorption techniques have been recently used in order to describe the exhaustion degree of granular activated carbons (GACs) using digital image processing techniques on X-Ray digital radiographies [4]. An X-ray image obtained from the exposition of the matter to the X-rays provides a shadow of intervening structures as a direct function of its density (σ) and atomic number (Z) [5, 6]. Digitalized X-ray image is a grey-scale matrix that can be in different formats depending on the nature of the image. For binaries or intensity images, image histogram constitutes a useful tool for analysing the characteristics of the resultant image, providing important information about the intensity levels and the total of pixels in the image [7–9]. Digital image processing by X-ray digital radiography have proved to be a suitable and sensitive tool to determine the GAC exhaustion degree [4]. Although neural networks have been widely applied in segmentation, classification and pattern recognition task [10–14], in X-ray images for medical diagnosis; deep learning techniques has not been applied yet to the characterization of the exhaustion degree of GACs. Deep learning techniques can be a powerful tool to enrich hand-engineered analysis, as X-Ray absorption method (XRA). When a large amount of data needs to be processed, XRA is more susceptible to errors, as it is demonstrated in this work. However, XRA limitations still are under investigation; therefore deep

✉ Jan Yperman, jan.yperman@uhasselt.be; Jeamichel Puente Torres, jeamichelp@gmail.com; Rafael Trujillo Codorniu, rtrujillo@uo.edu.cu; Rene López Baracaldo, rlopez@zimtronic.com; Harold Crespo Sariol, harold@uo.edu.cu; Thayset Mariño Peacok, thayset@uo.edu.cu; Peter Adriaensens, peter.adriaensens@uhasselt.be; Robert Carleer, robert.carleer@uhasselt.be; Ángel Brito Sauvanell, albrito@uo.edu.cu | [1]Faculty of Electrical Engineering, Universidad de Oriente, Santiago de Cuba, Cuba. [2]Zimtronic, Miami, FL, USA. [3]Faculty of Chemical Engineering, Energetic Efficiency Center, Universidad de Oriente, Santiago de Cuba, Cuba. [4]Research Group of Applied and Analytical Chemistry, Hasselt University, Agoralaan building D, 3590 Diepenbeek, Belgium.

SN Applied Sciences (2020) 2:2088 | https://doi.org/10.1007/s42452-020-03835-3

learning methods arises as an interesting tool for characterizing GACs.

A fundamental problem in machine learning is effective representation of complex inputs such as images or videos. Hand-engineered techniques have been popular in computer vision, and machine learning systems; based on these features, excellent results have been achieved on a variety of tasks [10–14]. However, these algorithms can be brittle, difficult to design, and inadequately representative in the use of high-dimensional inputs. Deep learning offers the promise of eliminating the dependence between extracted features from hand-designed algorithms, allowing directly learning from data. Until recently, most machine learning and signal processing techniques had exploited shallow-structured architectures. These architectures typically contain at most one or two layers of nonlinear feature transformations. Shallow architectures have been shown effective in solving many simple or well-constrained problems, but their limited representational power and poor modelling can cause difficulties when dealing with more complex real-world applications. This suggest that in order to deal with these kinds of problems one may need deep architectures. Neural networks with several hidden layers were difficult to train until the rise of convolutional neural networks (CNN) [15, 16]. A CNN is a kind of artificial neural network where neurons are related with receptive fields in a similar way to neurons behaviour in primary visual cortex of a biological brain. A CNN constitutes a variation in a multilayer perceptron, but its performance makes it more suitable in artificial vision tasks, especially for image classification. A CNN typically contains more than seven layers number that would be almost prohibitive for a fully connected network. CNN has obtained excellent results in visual recognition tasks applied to different areas as facial expressions recognition, digit classification [12, 16], satellite image classification [17], semantic image segmentation [16, 18] and object classification [19].

In this work, two methods based on deep neural networks are explored. Considering the effectiveness of CNN in image classification tasks, CNN architectures will be used as indirect methods for the detection of exhaustion degree of GAC samples using X-Ray digital radiographies (XRA). Both selected architectures show satisfactory results in GACs classification.

2 Materials and methods

2.1 GAC samples

GAC samples from a water purification system, to assist haemodialysis treatment (previously declared "out of operation" by exhaustion based on conductivity measurements) from a general hospital in Cuba, were used as first test sample [20]. Afterwards, GAC samples from an industrial filter (previously declared as "out of operation" by exhaustion based on rum master's criteria) from the major rum producer also in Cuba were used as second test samples to develop this study [4]. Figure 1 depicts schematics diagrams of both used filters.

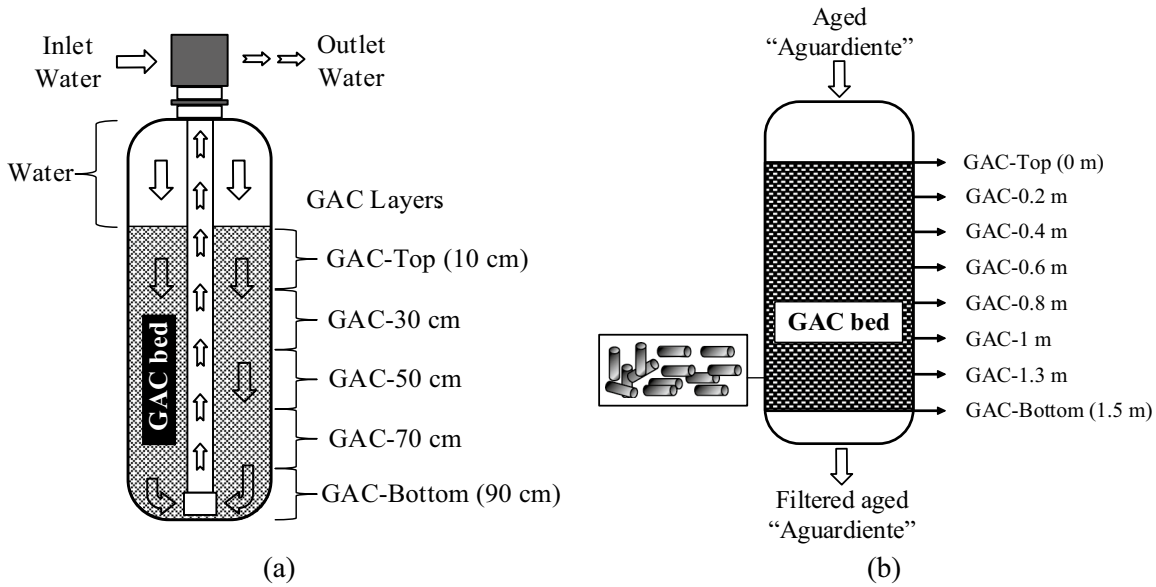

Fig. 1 Schematic diagram of the water treatment filter used for obtaining dialysis water for haemodialysis treatments and the samples locations at different layers in the GAC bed (**a**) and schematic diagram of the rum filter and the samples location from different GAC layers (**b**). (Adapted from [4, 20])

Recent studies prove that GAC samples extracted from the upper part of both filters (GAC-Top) usually are the region of the filter with the higher amount of adsorbed organic/inorganic compounds. Figure 1a depicts a schematic diagram of the water treatment filter used for obtaining dialysis water for hemodialysis treatments. Samples located at the upper part of the filter (GAC-Top 10 cm) were selected and used for this study. On the other hand, GAC samples also from the first GAC layer (GAC-Top 0 m) of industrial filter used in rum industry (Fig. 1b) completes the selected samples of exhausted GACs to be studied. Selected GAC samples were analysed using XRA and obtained images were used to carry out this work.

2.2 X-Ray absorption experiments (XRA)

XRA method is an innovative indirect method for characterizing GACs using X-Ray absorption images. Its physical principle uses the variations in X-Ray photoelectric absorption by GAC samples with different amounts of adsorbed compounds. The resulting radiographic image from the application of the XRA method as well as advance digital imaging processing techniques are used as evaluation criteria [4]. The digital radiographic image (as a grey scale representation of the X-ray absorption in the sample) contains information about the amount of adsorbed material in the GAC pores. The X-ray image parameters such as histograms, frequency spectrum, grey scale levels (GSI) and spatial concentration (Sc) can be used in order to have an idea of the exhaustion degree of the GACs with respect to a virgin GAC [4]. X-Ray digital radiographies were performed according to the methodology described in [4]. Briefly, an X-Ray beam source with an energy of 22 keV–125 mAs and a sample thickness of 12 mm were used. A TOSHIBA Mamorez-mgu 100d X-ray equipment used for mammography studies in manual mode (needed in order to adjust manually the energy of incident X-ray photons) was used to obtain digital radiographic images. Photoelectric effect is predominant in the energy range used for clinical X-Ray diagnosis (22 –120 keV); the law that rules the photoelectric attenuation can be expressed by the Eq. (1) [4–6].

$$N = N_0 e^{-\mu x} \tag{1}$$

where: N: Final Intensity or number of attenuated photons (dimensionless), N_0: Initial Intensity or number of incident photons (dimensionless), μ: Linear absorption coefficient (in mm^{-1}), x: Sample thickness (in mm)

It is possible to establish a direct relation between attenuated photons intensity (N) and the grey-scale intensity (GSI) values in the X-ray radiographic image [4]. This correlation can be mathematically expressed using Formula (2) [4].

$$GSI = f(N) \tag{2}$$

According to Eq. (2) it is possible to express GSI as an equivalent exponential function of the initial grey-scale intensity (GSI_0) using Formula (3) [4].

$$GSI = GSI_0 . e^{\mu . x} \tag{3}$$

where: GSI: Grey scale intensity of attenuated photons (in grey-scale levels), GSI_0: Grey scale intensity of incident photons (in grey-scale levels).

The XRA experiments and data processing of the X-ray digital images were performed following the images processing algorithm applied in [4]. In short, the X-ray image histograms of total pixels in a specific intensity level are expressed in a grey scale (GSI). Normalized grey scale intensity level in the discrete interval of [0 (black); 1 (white)] is used. The spatial concentration S_C (in pixel) describes the abundance of pixels at the same GSI value. The number of pixels for a specific GSI value can be related with the normalized grey scale value for the maximum of total of pixels, T_P(GSI), within this scale and can be expressed by Eq. (4) [4].

$$S_C(GSI) = T_P(GSI) \tag{4}$$

where: T_P(GSI): Total of pixels corresponding to GSI, S_C(GSI): Spatial concentration of the grey-scale intensity level GSI (in pixel).

The amount of X-Ray absorbed by a sample can be directly related with the density and atomic number of the material [5, 6]. The digital radiographic image (as a grey scale representation of the X-ray absorption in the sample) contains information about the amount of adsorbed material in the GAC pore. Then X-ray image parameters such as histograms, frequency spectrum and spatial concentration (Sc) can be used in order to have an idea of the exhaustion degree of used GAC with respect to virgin GAC [4]. A focal distance of 60 cm was used for all the experiments. The mathematical analysis of the digital X-Ray radiographic images is performed using dedicated software developed in MATLAB® specifically for this application. Images from TOSHIBA Mamorez-mgu 100d X-ray equipment were converted from DICOM to JPEG format.

2.3 Database description and data preparation

In order to obtain a significant set of images to develop the training process, original images (512 × 512 pixels) were subdivided into smaller images of 64 × 64 pixels; assuming that the exhaustion degree of each original sample should be reflected in each sub-image. However, image datasets

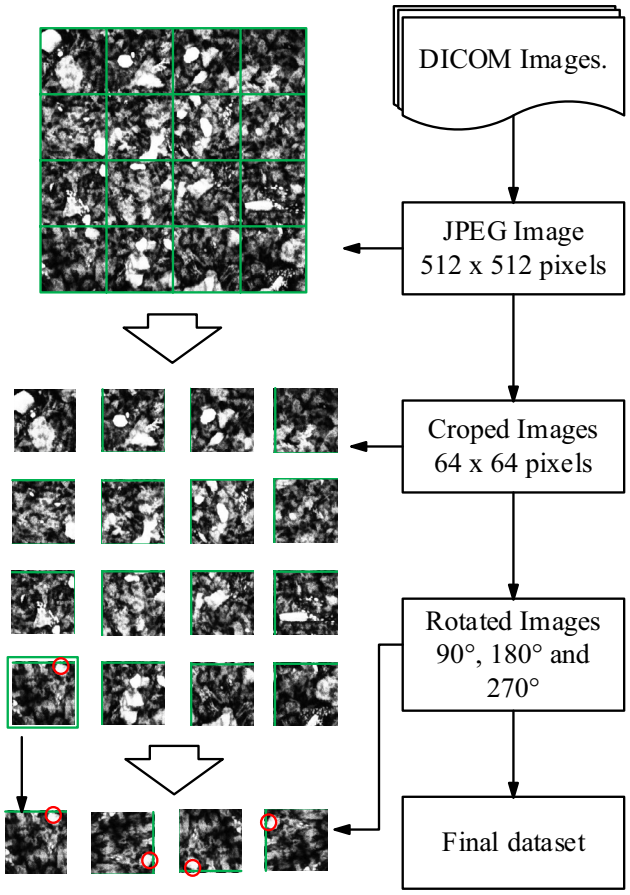

Fig. 2 Database preparation

designed for image classification tasks contain significantly more images per class for training than our dataset; therefore, a data augmentation process is applied by using class-preserving transformations of the original images. Figure 2 illustrates the procedure of data preparation.

In particular, rotations of 90°, 180° and 270° were applied, 32 exhausted images (512 × 512 pixels) were cropped into 64 × 64 pixels smaller images, getting 2048 images (32 × 64). After the cropping process, rotations are applied, obtaining 8192 images (2048 × 4); 464 images of 64 × 64 pixels are added to the initial amount, using original images of variable size. A similar process was applied for virgin images (in this case completed with 560 images of 64 × 64 pixels from original virgin images of variable size); getting a final dataset with 17,408 (virgin images added to exhausted images) images: 8752 (8192 + 560) images were labelled as virgin GAC and 8656 (8192 + 464) as exhausted GAC. Variable size images were cropped until square crops of 64 × 64 pixels were possible. From the original dataset of 17,408 images, 16,000 were randomly selected to be used in the training process and the remainder 1408 images were used in a validation process. For the training process, 8000 images correspond to exhausted GAC and the remainder 8000 images to virgin GAC. For the validation process 1408 images, 656 and 752 exhausted and virgin images, were used.

2.4 Work environment

Experiments were performed using the framework Keras 2.0 with Python 2.7. The computer used was equipped with a HP motherboard with 8 GB RAM, an Intel (R) Xeon (R) ES-1620 processor with 8 cores. The graphics-processing unit used was a NVidia GeForce GTX-980 with 4 GB of RAM and 2048 CUDA cores. Computer operative system was Window 10.

2.5 Net definition

Two architectures are proposed; both have its foundations in convolutional networks [13, 15, 16]. XRA-2D network is a classical CNN with 22 layers inspired in VGG16 network, with blocks that use two or three 3 × 3 convolutions followed by a max-polling. However, the number of used channels for the convolutions is significantly lower compared with VGG16 network. XRA-2D architecture is depicted in Fig. 3. Two convolutional layers, a

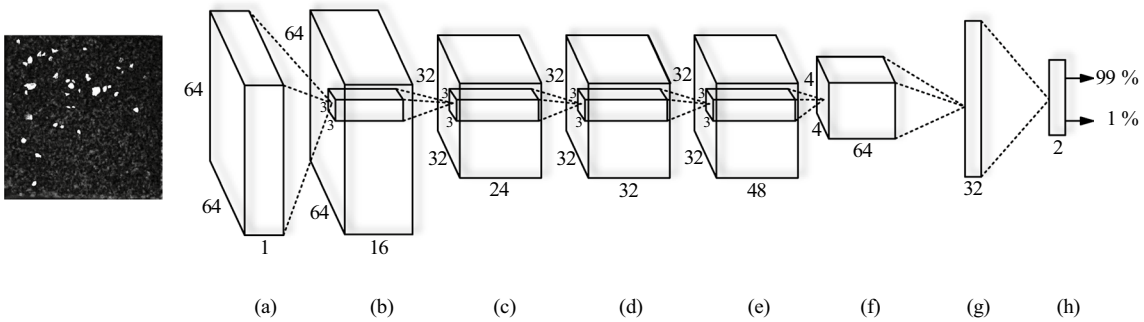

Fig. 3 CNN network XRA-2D. Original image of 64 × 64 pixels in grey-scale (a). First convolution block with 3 × 3 filters and 16 channels (b). Convolutions blocks with 24, 32, 48 and 64 channels respectively (c), (d), (e) and (f). Dense layer with 32 neurons with dropout (g). Dense final layer with two outputs (h)

sub-sampling layer and a dropout layer are conforming the blocks (b), (c), (d), (e) and (f). At each output of (b), (c), (d), (e) and (f) blocks, image dimension is reduced to the half.

Each unit in a convolution layer receives input from a set of units located in small neighbourhood in the previous layer. All convolutional layers in XRA-2D have receptive fields equal to 3 × 3 pixels. With local receptive fields, neuron, can extract elementary visual features such as edges, corners, etc. These features are then combined in subsequent layers in order to detect higher-order features.

The sub-sampling layer takes a small rectangular block of the previous convolutional layer and develops a sub-sampling process in order to obtaining a simple output from the block. This process can be performed using several techniques: (1) using the mean of the neurons from the block [17], (2) using the maximum value [12]; or (3) using a linear combination. It has been demonstrated that using the maximum value from the block (max pooling), it is more efficient in order to summarize region characteristics [18]. Max pooling operations has similarities with the biological behaviour of visual cortex and how it is capable of summarize information [19]. Max pooling operation causes a reduction in data size in a factor equal to the size of the sample window on which the operation has been developed.

Finally, the dropout layer sets the output of each neuron to zero with a certain probability p (0.25 in XRA-2D network) on each iteration of training [21]. Developing this operation, the risk of overfitting in the network is attenuated. The overfitting in automatic learning is the effect of overtraining a learning algorithm; then, algorithms are learning about peculiarities of the training set without understanding the features well enough to generalize to the validation set.

Two last layers in XRA-2D network are dense (fully connected) (Fig. 3g, h) classification layers (at this point original image is not an image anymore). The last layer (h) provides two outputs that could be interpreted as the probability in which the original image (64 × 64 pixels) can be classified as an image from an exhausted or virgin GAC. Probability values can be used to have an idea of the exhaustion degree of a GAC. Typical CNN2D classifiers always expect an input of the same size. Taking this into account, modification in original images dimensions were applied in order to evaluate XRA-2D network performance by reducing its original size to 64 × 64 pixels.

The second network used (XRA-1D) is based in the hypothesis exposed in [4], were image histograms and S_C concept can be used to detect changes in exhaustion degree between GACs. Considering this hypothesis, a 64 bins image histogram (from the original image of 64 × 64 pixels) is introduced at the input of XRA-1D network. Figure 4 depicts XRA-1D architecture.

Using images histograms reduces data dimensions, making the architecture of XRA-1D network simpler in comparison with XRA-2D network. The use of histograms and its combination with convolutional layers has been used before with reliable results [22]. Two convolution layers, a sub-sampling layer and a dropout layer (as in XRA-2D network) are conforming each convolution block showed in Fig. 4. The dropout layers disconnection ratio is about 25%, allowing to obtaining reliable results. In XRA-2D and XRA-1D networks the "LeakyRelu" function [23] is used as neural activation function in all the layers except in the last layer where the function "softmax" is used.

In both networks (XRA-2D and XRA-1D), at least 20 training epochs were used, rearranging the images on mini-batches of 25 images each one. The loss function ("binary cross entropy") was used as objective function and as optimization algorithm "RMSProp" was selected [24]. Weights initialization and "RMSProp" parameters were obtained by default using Keras framework.

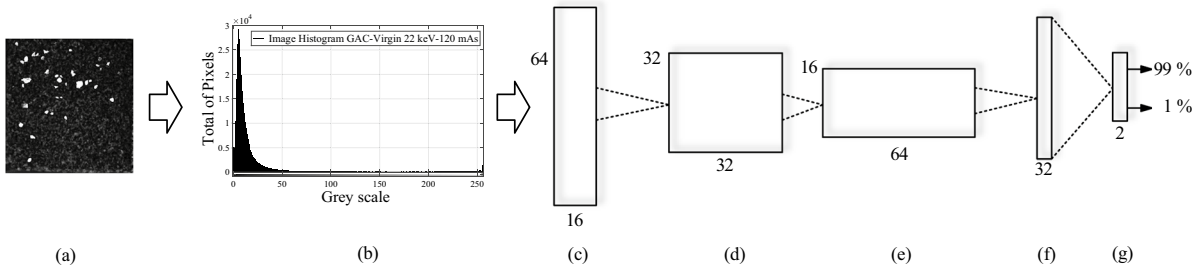

Fig. 4 CNN network XRA-1D. Original image of 64 × 64 pixels in grey-scale (a). Image histogram with 64 bins from original image (b). Convolutions blocks with 16, 32 and 64 channels respectively (c), (d) and (e). Dense layer with 32 neurons with dropout (f). Dense final layer with two outputs (g)

3 Results and discussion

3.1 Quantitative results

From obtained dataset (cropped images), some images were incorrectly classified; indicating that probably the exhausted GAC reflected in original images were not necessarily manifested in a homogeneous way in cropped images (64 × 64 pixels). Figure 5 shows a set of images incorrectly classified.

Figure 6 shows the evolution of loss function in training process.

The loss function is better at epoch 19 in training process for XRA-2D network (Fig. 6a). A success rate of 97.7% is obtained for XRA-1D network, reinforcing the hypothesis that, in this case, using image histogram not only decrease architecture complexity, but also improves its classification capacity. A much more monotonous decline in the loss function is found for XRA-1D (Fig. 6b) network in comparison with XRA-2D, reinforcing the goodness of the use of images histograms from XRA method in order to design network architecture.

3.2 Comparison with XRA

Obtained database for training (16,000 images) was evaluated considering image histograms, grey-scale intensity levels and S_C concept, 8000 images from exhausted and virgin GAC dataset were analysed using the histogram criteria. It has been demonstrated in recent publications [4] that image histograms from exhausted GACs present GSI values upper 0.38 in normalized grey scale. On the other hand, image histograms from virgin GAC present GSI values under 0.1 in normalized grey scale [4]. Previous criteria are applicable only when 22 keV–125 mAs (voltage and intensity), 12 mm of sample thickness and 60 cm of focal distance are applied to analyse the sample using XRA method. Using the previous criteria, 720 images from exhausted images dataset were classified as virgin

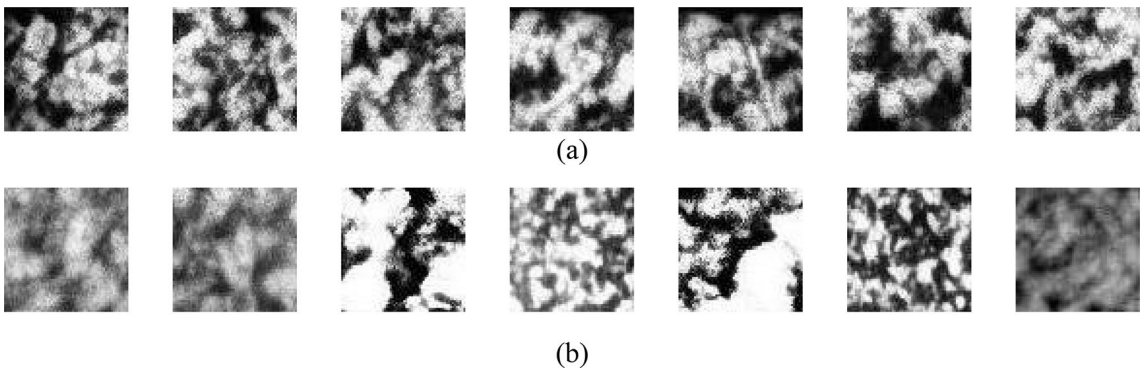

Fig. 5 Images incorrectly classified; (**a**) images (64 × 64 pixels) from an exhausted GAC predicted as a virgin GAC and (**b**) images (64 × 64 pixels) from virgin GAC predicted as an exhausted GAC

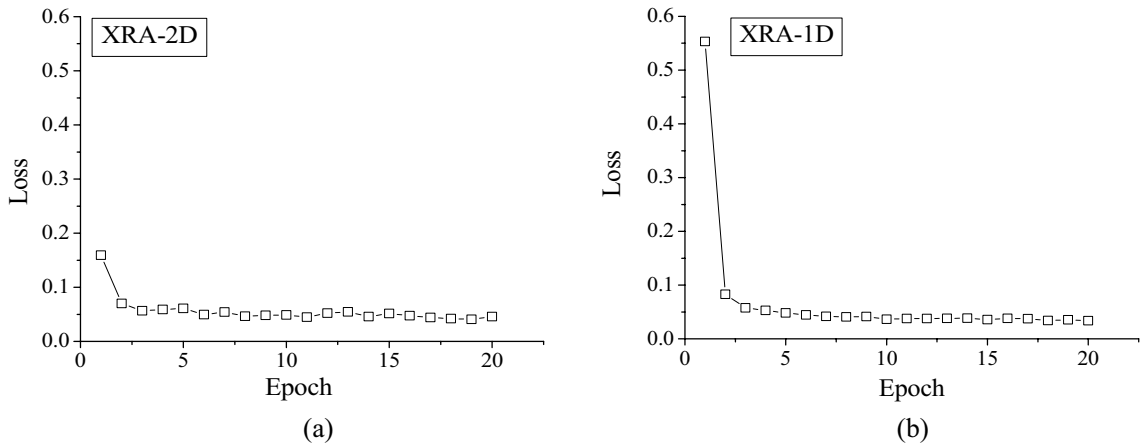

Fig. 6 Loss function for training in XRA-2D (**a**) and XRA-1D (**b**) network for each training epoch respectively

Table 1 Accuracy of used methods for the detection of exhausted GACs

Method	XRA2D network (%)	XRA1D network (%)	XRA (histogram) (%)
Accuracy (original images)	100	100	98
Accuracy (cropped images)	97.4	97.7	91

sample; giving to histogram criteria a 91% of success when it is applied on exhausted images (64 × 64 pixels). In using original exhausted images (512 × 512 pixels), a 98% of success is achieved. When XRA dataset from virgin samples is analysed, 2638 images are classified as exhausted samples, giving in this case a success rate of 67% approximately when histogram criteria are applied on images (64 × 64 pixels) from virgin GAC. Table 1 depicts a comparison between used methods to detect exhausted GACs.

A success rate of 100% is achieved when original virgin GAC images are analysed (all the results showed in Table 1 are obtained using validation sets). This phenomenon reinforces the hypothesis formulated in Sect. 3.1. Nevertheless, both designed architectures (XRA-2D and XRA-1D) are capable to obtain success rates around 97% using the dataset for exhausted images (cropped images) and 100% success rates when original images are analysed. On the other hand, when the number of images increases XRA (histogram) criteria is only capable to achieve success rates of 98% for original images and 91% for cropped images.

4 Conclusions

In this work, two new CNN architectures for determination of exhaustion degree of GACs based in X-Ray absorption images from the application of XRA method are proposed.

Both architectures are capable to achieve satisfactory success rates in differentiating exhausted GAC from a virgin GAC determining the exhaustion degree of GACs samples through a dataset of images obtained applying XRA method. XRA-1D network shows the best performance. Obtained results indicates that the use of deep learning algorithms is more adequate to analyse a large amount of data in comparison with XRA method.

The application of neural networks technology through XRA-2D and XRA-1D architectures opens the possibility of application of deep learning algorithms in the assessment of other porous materials using digital radiographic images obtained applying XRA method.

Acknowledgements The authors would like to thank UH-BOF funding and VLIR-UOS (Flemish Interuniversity Council for University Development Cooperation) project between Belgium and Cuba for providing funding and granting the support of the current and future studies.

Compliance with ethical standards

Conflict of interest The author(s) declare that they have no competing interests.

References

1. Bansal CR, Goyal M (2005) Activated carbon adsorption. Taylor & Francis, New York
2. Hsieh CT, Teng HS (2000) Influence of mesopore volume and adsorbate size on adsorption capacities of activated carbons in aqueous solutions. Carbon 38:863–869
3. Ying WC (1989) Proceedings of the 44th Purdue industrial waste conference. Lewis Publishers, Chelsea, MI, p 313
4. Puente Torres J, Crespo Sariol H, Yperman J, Brito Sauvanell A, Carleer R, Navarro Campa J (2018) A novel X-Ray radiography approach for the characterization of granular activated carbons used in rum production. J Anal Sci Technol 9(1):1–15
5. Cherry RN Jr (1993) Ionizing radiations. American National Standards Institute (ANSI), New York
6. Robert Cunningham J (1986) The physics of radiology. Charles C Thomas Publisher, Springfield, IL
7. Gonzales RC, Woods RE (2002) Digital image processing, 2nd edn. Prentice Hall, Upper Saddle River, NJ
8. Gonzales RC, Woods RE, Eddins SL (2004) Digital image processing using Matlab. Prentice Hall, Upper Saddle River, NJ
9. Semmlow JL (2004) Biosignal and biomedical image processing. Marcel Dekker, New York
10. Dalal N, Triggs B (2005) Histograms of oriented gradients for human detection. Comput Vis Pattern Recogn 1(25):886–893
11. Lowe DG (2004) Distinctive image features from scale invariant keypoints. Int J Comput Vis 60(2):91–110
12. LeCun Y, Bottou L, Bengio Y, Haffner P (1998) Gradient-based learning applied to document recognition. Proc IEEE 86(11):2278–2324
13. Sermanet P, Chintala S, LeCun Y (2012) Convolutional neural networks applied to house numbers digit classification. arXiv preprint arXiv 1204.3968
14. Nguyen PD. Astaxanthin: a comparative case of synthetic vs natural production. Chemical and Biomolecular Engineering. http://trace.tennessee.edu/utk_chembiopus
15. Krizhevsky A, Sutskever I, Hinton EG (2012) ImageNet classification with deep convolutional neural networks. Adv Neural Inform Process Syst 2012:1097–1105
16. Long J, Shelhamer E, Darrell T (2015) Fully convolutional networks for semantic segmentation. In: Proceedings of the IEEE conference on computer vision and pattern recognition, pp 3431–3440
17. Lin M, Chen Q, Yan S (2014) Network in network. International Conference on Learning representations abs/1312.4400
18. Chang JR, Chen YS (2015) Batch-normalized maxout network in network. arXiv preprint arXiv 1511.02583
19. Desimone R, Ducan J (1995) Neural mechanisms of selective visual attention. Annu Rev Neurosci 18(1):193–222
20. Puente Torres J et al (2019) X-Ray absorption as an alternative method to determine the exhausting degree of activated carbon layers in water treatment system for medical services. Talanta 205:120058

21. Srivastava N, Hinton G, Krizhevsky I, Ruslan S (2014) Dropout: a simple way to prevent neural networks from overfitting. J Mach Learn Res 15(1):1929–1958
22. Chen M, Sedighi V, Boroumand M, Fridrich J (2017) JPEG-phase-aware convolutional neural network for steganalysis of JPEG images. In: Proceedings of the 5th ACM workshop on information hiding and multimedia security, pp 75–84
23. Maas LA, Hannun YA, Ng AY (2013) Rectifier nonlinearities improve neural network acoustic models. Proc ICML 30(1):3
24. Hinton EG (2012) A practical guide to training restricted Boltzmann machines. In: Neural networks: tricks of the trade. Springer, Berlin, pp 599–619